

RESEARCH

Open Access



# Host genetics and gut microbiota influence lipid metabolism and inflammation: potential implications for ALS pathophysiology in SOD1<sup>G93A</sup> mice

Elena Niccolai<sup>1</sup>, Leandro Di Gloria<sup>2</sup>, Maria Chiara Trolese<sup>3</sup>, Paola Fabbrizio<sup>3</sup>, Simone Baldi<sup>1</sup>, Giulia Nannini<sup>1</sup>, Cassandra Margotta<sup>3</sup>, Claudia Nastasi<sup>4</sup>, Matteo Ramazzotti<sup>2</sup>, Gianluca Bartolucci<sup>5</sup>, Caterina Bendotti<sup>3</sup>, Giovanni Nardo<sup>3\*</sup> and Amedeo Amdei<sup>1\*</sup>

## Abstract

Amyotrophic Lateral Sclerosis (ALS) is a devastating neurodegenerative disorder characterized by the progressive loss of motor neurons, with genetic and environmental factors contributing to its complex pathogenesis. Dysregulated immune responses and altered energetic metabolism are key features, with emerging evidence implicating the gut microbiota (GM) in disease progression. We investigated the interplay among genetic background, GM composition, metabolism, and immune response in two distinct ALS mouse models: 129Sv\_G93A and C57Ola\_G93A, representing rapid and slow disease progression, respectively.

Using 16 S rRNA sequencing and fecal metabolite analysis, we characterized the GM composition and metabolite profiles in non-transgenic (Ntg) and SOD1<sup>G93A</sup> mutant mice of both strains. Our results revealed strain-specific differences in GM composition and functions, particularly in the abundance of taxa belonging to Erysipelotrichaceae and the levels of short and medium-chain fatty acids in fecal samples. The SOD1 mutation induces significant shifts in GM colonization in both strains, with C57Ola\_G93A mice showing changes resembling those in 129 Sv mice, potentially affecting disease pathogenesis. ALS symptom progression does not significantly alter microbiota composition, suggesting stability.

Additionally, we assessed systemic immunity and inflammatory responses revealing strain-specific differences in immune cell populations and cytokine levels.

Our findings underscore the substantial influence of genetic background on GM composition, metabolism, and immune response in ALS mouse models. These strain-specific variations may contribute to differences in disease susceptibility and progression rates. Further elucidating the mechanisms underlying these interactions could offer novel insights into ALS pathogenesis and potential therapeutic targets.

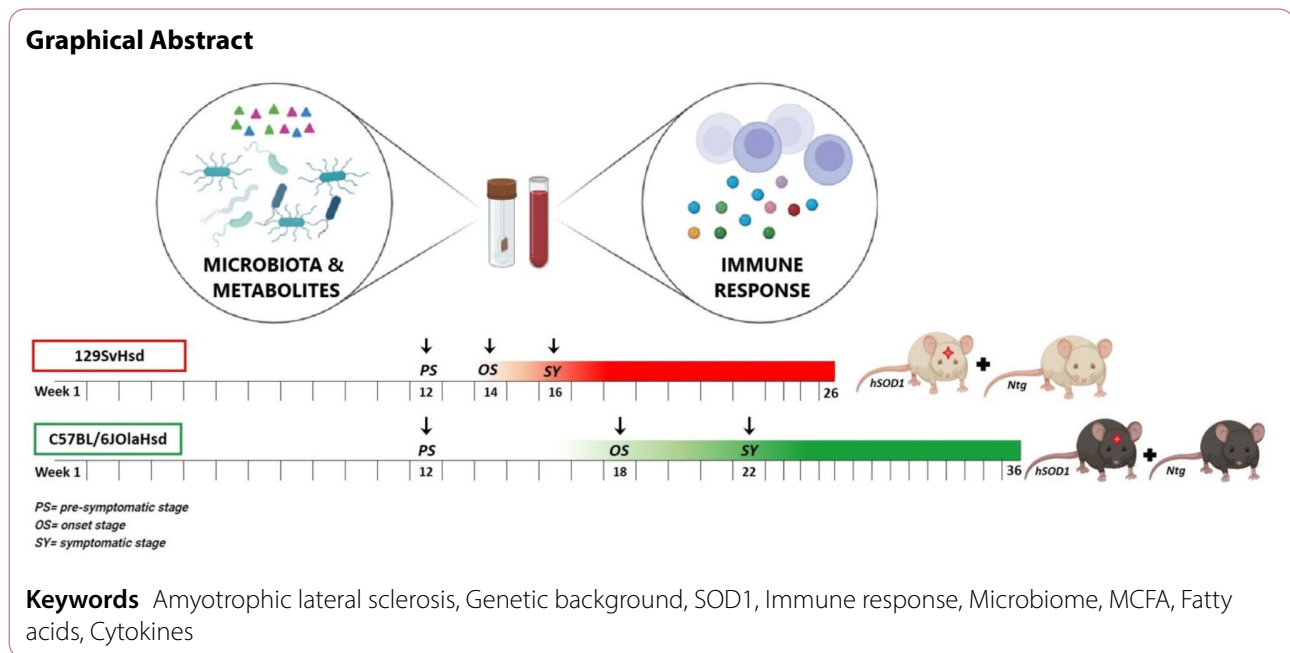
\*Correspondence:

Giovanni Nardo  
giovanni.nardo@marionegri.it  
Amedeo Amdei  
amedeo.amedei@unifi.it

Full list of author information is available at the end of the article



© The Author(s) 2024. **Open Access** This article is licensed under a Creative Commons Attribution-NonCommercial-NoDerivatives 4.0 International License, which permits any non-commercial use, sharing, distribution and reproduction in any medium or format, as long as you give appropriate credit to the original author(s) and the source, provide a link to the Creative Commons licence, and indicate if you modified the licensed material. You do not have permission under this licence to share adapted material derived from this article or parts of it. The images or other third party material in this article are included in the article's Creative Commons licence, unless indicated otherwise in a credit line to the material. If material is not included in the article's Creative Commons licence and your intended use is not permitted by statutory regulation or exceeds the permitted use, you will need to obtain permission directly from the copyright holder. To view a copy of this licence, visit <http://creativecommons.org/licenses/by-nc-nd/4.0/>.



## Introduction

Amyotrophic Lateral Sclerosis (ALS), a neurodegenerative disorder characterized by the progressive loss of motor neurons, entails a multifaceted interplay of genetic and environmental factors, underpinning its diverse clinical manifestations [25]. This complexity is marked by substantial genotypic and phenotypic heterogeneity, extending beyond motor neurons. This variability underscores the complexity of the disease and highlights the need for comprehensive investigations to unravel its underlying mechanisms [29]. The pathophysiology of ALS implicates a dysregulated immune system, evidenced by neuroinflammation, involving both resident and peripheral immune cells, which contributes to disease progression [5, 18]. Central and peripheral inflammatory mechanisms are significant contributors to ALS, both in the context of specific genetic mutations and probably as a consequence of the general disease process in sporadic cases [17, 47]. However, the role of the immune system in ALS is complex; initially protective responses are eventually overridden by cytotoxic processes [5, 48]. Another significant aspect of ALS pathology involves the alteration of energetic metabolism, particularly lipid metabolism, exacerbating its complexity [48]. In many patients, there is evidence of a hypermetabolic state that correlates with a more severe lower motor neuron involvement, accelerated functional decline, and shorter survival times [10]. Skeletal muscles suggested as the origin site of this metabolic alteration, exhibit increased energy demand due to chronic denervation, further exacerbating fat mass depletion [40]. Furthermore, ALS is characterized by alterations in plasma lipid levels and changes in fatty

acid  $\beta$ -oxidation [8, 64]. Interestingly, hyperlipidemia is associated with increased survival rates, possibly due to the protective effect of elevated lipid levels in circulation [22]. The exact mechanisms underlying hyperlipidemia in ALS remain unclear but could involve mitochondrial dysfunction [23].

Such intricacies prompt exploration into potential contributors, including the gut microbiota (GM) and its modulation of metabolism and immune responses. GM has garnered attention in neurological conditions for its capacity to influence brain function and disease progression. Evidence has implicated GM dysbiosis in driving ALS features and progression, both in patients and in animal models [7, 11, 20, 27, 53]. Notably, previous studies in superoxide dismutase 1 (SOD1) transgenic mice, an established ALS animal model, have unveiled alterations in the gut barrier, abnormal Paneth cell presence, and changes in gut microbial composition, implicating the GM in ALS [63, 69]. Moreover, alterations of microbial metabolites may affect ALS by immune cell activation or cell polarization (regulatory versus effector cells) possibly sustaining neuroinflammation and neuron degeneration [45]. Furthermore, GM contributes significantly to regulating the energetic metabolism, suggesting another potential association between GM and disease progression [45]. For instance, the GM plays a role in converting primary bile acids into secondary bile acids, which are essential for lipid digestion in the gastrointestinal tract and interact with receptors that regulate host metabolism. Additionally, GM composition influences the levels of free fatty acids (FFAs) in the body, serving as essential energy sources for tissues and regulators of the

inflammatory response [37]. Studies conducted in SOD1 mice have demonstrated significant metabolic dysfunction associated with changes in GM composition [61]. Moreover, Guo and colleagues have recently found disparities in the GM composition between ALS cases and controls, with correlations observed between specific genera and plasma metabolites, particularly lipids [32]. These insights underscore the potential significance of GM-mediated metabolic alterations in ALS pathogenesis, suggesting avenues for further exploration into the intricate interplay between gut health, metabolic dysregulation, and neurodegeneration in this devastating disease.

Transgenic mice expressing various human SOD1 mutations closely mimic clinical and pathological features of human ALS, including significant phenotypic variability in terms of onset age and disease progression speed [6, 35]. Particularly intriguing are mice carrying the SOD1<sup>G93A</sup> transgene on different strains [51]. Despite expressing the same quantity of the human mutant SOD1 protein [41, 42], those on 129SvHsd genetic background (129Sv\_G93A, denoted as fast-progressing) exhibit a considerably swifter disease course compared to those on the C57BL/6JOLA Hsd background (C57Ola\_G93A, slow-progressing), underscoring the substantial influence of genetic background on modulating ALS progression [57]. Transcriptomic analyses of laser-dissected lumbar motor neurons have further highlighted significant gene expression differences in pathways related to metabolism, protein degradation, and immune response [50]. In addition, metabolomic analysis of the spinal cord of two mouse strains evidenced substantial metabolic effects relating to genetic background which may contribute to ALS progression differences between the two SOD1G93A strains [68]. More recently, we demonstrate an important influence of the immune response in determining the different onset and progression of the disease in these mice [41, 66].

Given the bidirectional impact of immunity on the composition and function of the microbiota, our study delved into the influence of genetic background on the composition of the GM, the fatty acid metabolism and the immune response in fast and slow-progressing SOD1<sup>G93A</sup> mouse models. Our findings unraveled the intricate interconnections of these biological processes that may contribute to the nuanced landscape of ALS progression and its variability.

## Materials and methods

### Animals management and sample collection

Female transgenic 129SvHsd (129Sv\_G93A) ( $n=8$ ), C57BL/6JOLA Hsd (C57Ola\_G93A) ( $n=8$ ) and their corresponding non-transgenic littermates ( $n=10$  and  $n=8$ , respectively) have been used in this study. Mice have been maintained at a temperature of  $21\pm 1$  °C with a

relative humidity of  $55\pm 10\%$  and a 12 h light/dark cycle. Food (standard pellets) and water will be supplied ad libitum. Procedures involving animals and their care has been conducted according to the Mario Negri institutional guidelines, which are compliant with national (D.L. no. 116, G.U. suppl. 40, Feb.18, 1992, Circular No.8, G.U., 14 July 1994) and international policies (EEC Council Directive 86/609, OJ L 358, 1 Dec.12, 1987; NIH Guide for the Care and use of Laboratory Animals, U.S. National Research Council, 1996). All experiments and protocols will be examined by the Institutional Ethical Committee and authorized by the Italian Ministry of Health. The mice have been bred and maintained in a specific pathogen-free environment. Animals with substantial motor impairment had food on the cage bottom and water bottles with long drinking spouts.

Blood and faeces have been collected from 129Sv\_G93A mice or C57Ola\_G93A mice and age-matched Ntg littermates at pre-symptomatic (PS=12 weeks for both models), onset (OS=14 or 18 w age, respectively) and symptomatic (SY=16 or 22 w age, respectively) stage. To avoid any bias, mice were separated by strain (C57Ola Vs. 129 Sv) and genotype (NTg Vs. SOD1G93A) (No. 4 per cage) and sampling was done per mouse by taking fresh blood and faeces at the defined timepoints.

### Faecal microbiota characterization

Total DNA was extracted using the DNeasy PowerLyzer PowerSoil Kit (Qiagen, Hilden, Germany) from frozen ( $-80$  °C) stool samples, according to the manufacturer's instructions. Briefly, 0,25 g of stool samples were added to a bead beating tube and homogenized with TissueLyser II for five minutes at 30 Hz. Genomic DNA was captured on a silica membrane in a spin column format, washed and subsequently eluted. The quality and quantity of extracted DNA were assessed with the Qubit Fluorometer (Thermo Fisher Scientific) and then frozen at  $-20$  °C.

Subsequently, DNA samples were sent to IGA Technology Services (Udine, Italy) where amplicons of the variable V3–V4 region of the bacterial 16s rRNA gene, obtained through primers 341 F and 805R, were sequenced in paired-end ( $2\times 300$  cycles) on the Illumina MiSeq platform, according to the Illumina 16 S Metagenomic Sequencing Library Preparation protocol.

The demultiplexed sequence reads were processed in QIIME2 2022.8 environment. Briefly, the sequencing primers and the reads without primers were removed using the Cutadapt tool. DADA2 was used to perform paired-end reads filtering, merging and chimeras' removal steps after trimming low-quality nucleotides from both forward and reverse reads ( $--p-trunc-len-f$  274  $--p-trunc-len-r$  169). Hence, ASVs (amplicon sequence variants) were generated, and the taxonomic

assignments were performed through the Scikit-learn multinomial naive Bayes classifier re-trained on SILVA database (release 138) V3-V4 hyper-variable region. Every cross-amplified host DNA has been identified and removed, aligning the ASVs to GRCm39 (murine reference genome) using Bowtie2 2.2.5. Moreover, the ASV derived from chloroplasts or mitochondria, according to SILVA, were also discarded. Finally, every ASV associated with genera with mean relative abundance across the samples under the cutoff of 0.005% have been discarded to minimize sequencing contaminants and improve statistical inferences [9, 12]. Finally, the potential expression of microbial pathways in each sample were estimated using PICRUSt2 v 2.5. Further details about the FASTQ processing are available at [https://github.com/LeandroD94/Papers/tree/main/2024\\_SLA\\_mice\\_Fast129Sv\\_SlowC57\\_G93A](https://github.com/LeandroD94/Papers/tree/main/2024_SLA_mice_Fast129Sv_SlowC57_G93A).

#### Short and medium chain fatty acids analysis

The evaluation of short and medium chain fatty acids (SCFA and MCFA, respectively) and the standard curves' preparation was performed on stools of 12 weeks age mice, by an Agilent GC-MS system composed of a 5971 single quadrupole mass spectrometer, 5890 gas chromatograph and 7673 autosampler, through our previously described GC-MS method [52].

#### Immunophenotype analysis in blood

Peripheral blood mononuclear cells (PBMCs) were isolated from whole blood with Lymphosep (L0560, Biowest) according to manufacturer instructions and stained with the following antibodies: BUV 661 rat anti-mouse CD45 (612975, BD Biosciences), BUV395 rat anti-CD11b (563553, BD Biosciences), BV421 anti-mouse Ly6G (127627, Biolegend) and FITC anti-mouse Ly6C (128005, Biolegend). Events were acquired with Cytotflex LX (Beckman Coulter) using the gating strategy showed in the Figure S4. Flow cytometry data were analyzed using FlowJo™ v10.8 Software (BD Life Sciences).

#### Molecular inflammatory response evaluation

Serum cytokines (IL-1β, IL-6, IL-17, KC/IL-8, monocyte chemoattractant protein 1 (MCP-1) and, tumor necrosis factor-α (TNF α)) were assayed in 5 mice/group using the Milliplex Map kit Mouse cytokine/chemokine magnetic bead panel for the Luminex MAGPIX detection system (Merck) following the manufacturer's instructions. Cytokine levels were estimated using a 5-parameter polynomial curve with Bio-plex Manager software (Biorad).

#### Statistical analyses

Continuous variables were presented as median value and interquartile range (calculated as the difference

between the 75th and 25th percentiles of the data) and were compared using the non-parametric Mann-Whitney test.

The statistical analyses on bacterial communities were performed in R 4.3 with the help of the packages phyloseq 1.44.0, vegan 2.6-4, DESeq2 1.40.1 and other packages satisfying their dependencies. The packages ggplot2 3.4.2, ggh4x 0.2.2 and ggpubr 0.40 were used to plot data and results. A saturation analysis on ASV was performed on every sample using the function rarecurve (step 50 reads), further processed to highlight saturated samples (arbitrarily defined as saturated samples with a final slope in the rarefaction curve with an increment in ASV number per reads < 1e-5). The observed richness and Shannon indices were used to estimate the bacterial genera alpha-diversity in each sample using the function estimate\_richness from phyloseq. The Pielou's evenness index was calculated using the formula  $E = S / \log(R)$ , where S is the Shannon diversity index, and R is the observed ASV richness in the sample. Differences in alpha-diversity indices were inspected through the Mann-Whitney test. PCoAs were performed using the Hellinger distance on Hellinger transformed genera abundances. PERMANOVA and Betadisper were used to test the statistical significance of the beta-diversity distances and dispersions. At different taxonomic ranks, the differential analysis (DA) of the abundances has been computed with DESeq2 on raw count data, and only the results with a *p*-value (adjusted through Benjamini-Hochberg method) lower than 0.01 were considered significant. Furthermore, differentially abundant taxa with a DESeq2 baseMean value lower than 100 have been discarded from the displayed results, irrespective of their statistical significance, to limit noisy results. Finally, the algorithm Lefse v 1.1.2 was utilized to compare the expression of microbial pathways predicted by PICRUSt2 between genotypes and strains. Spearman correlation coefficients were calculated to evaluate the association between fatty acids and bacterial taxa; *p*-values were corrected for multiple comparisons using the Benjamini-Hochberg FDR procedure. Further details about the analyses regarding the microbiota are available at [https://github.com/LeandroD94/Papers/tree/main/2024\\_SLA\\_mice\\_Fast129Sv\\_SlowC57\\_G93A](https://github.com/LeandroD94/Papers/tree/main/2024_SLA_mice_Fast129Sv_SlowC57_G93A).

## Results

### Distinct microbiota profiles in non-transgenic C570la and 129 sv strains

The sequencing efforts in assessing microbiota composition encompassed a total of 13,650,526 reads for 101 samples. After all the steps of pre-processing (pair merging, trimming, quality filtering, chimera detection) and decontamination, a total of 6,969,470 (51%) were available for further analysis. Saturation curves revealed that every specimen was sufficiently sampled (Figure S1).

Samples showed a Good's coverage ranging from 99 to 100%, indicating that less than 1% of the reads in a given sample came from ASVs, that appeared only once in that sample. The subsequent taxonomic analysis, detailed in Table S1, identified nine phyla, 12 classes, 26 orders, 41 families and 89 genera. In all samples, the top five phyla exhibited the following average abundances: Firmicutes (47.9%), Bacteroidota (40.2%), Campilobacterota (6.2%), Desulfobacterota (1.8%), and Actinobacteriota (1.3%) (Figure S2A). The ten most abundant genera were *Muribaculaceae* (27.2%), *Lactobacillus* (21.3%), *Helicobacter* (6.2%), an *unidentified genus* of Lachnospiraceae family, (4.3%), *NK4A136\_group* of Lachnospiraceae (3.9%), *Dubosiella* (3.7%), *Alistipes* (2.9%), *Bacteroides* (2.8%), *Odoribacter* (2.5%), and an uncultured genus of Lachnospiraceae (2.1%) (Figure S2B).

The microbiota composition between non transgenic C57Ola and 129 Sv strains exhibited notable distinctions. Specifically, at 12 weeks of age, C57OlaNtg and 129SvNtg mice displayed divergent microbiota profiles. Analysis of alpha diversity indicated that in the 129 Sv strain, the microbiota did not exhibit a significantly higher ASV richness but a greater abundance uniformity as evidenced by the Evenness index ( $p=0.034$ ) compared to the

C57Ola strain (Fig. 1A). More importantly, beta diversity analysis revealed a highly significant separation in microbiota composition between the two strains, as demonstrated by a very low  $p$ -value in the PERMANOVA test ( $p=0.0001$ ) (Fig. 1B), highlighting the distinct microbial communities associated with each genetic background.

In-depth univariate analysis disclosed differences in abundances at specific taxonomic levels. Within these disparities, the 129SvNtg mice exhibited a notable increase in Clostridia ( $\log_2FC=-1.41$ ,  $padj=0.006$ ) and genera belonging to the Lachnospiraceae family, such as *Roseburia* ( $\log_2FC=-2.52$ ,  $padj=0.0006$ ), an *unidentified genus* of Lachnospiraceae clade ( $\log_2FC=-1.9$ ,  $padj=0.0015$ ), and A2 genus ( $\log_2FC=-5.35$ ,  $p<0.0001$ ) compared to C57OlaNtg. Conversely, there was a decrease in the Erysipelotrichaceae family (Bacilli) ( $\log_2FC=6.01$ ,  $p<0.0001$ ), especially *Dubosiella* ( $\log_2FC=14.92$ ,  $p<0.0001$ ) and *Faecalibaculum* ( $\log_2FC=12.46$ ,  $p<0.0001$ ) genera, and in the Coriobacteriaceae *UCG-002* genus ( $\log_2FC=9.93$ ,  $p<0.0001$ ) (Fig. 1C). We also detect differences in the fecal levels of short and medium-chain fatty acids. In detail, the percentage of total MCFAs ( $p=0.041$ ), heptanoic acid ( $p=0.049$ ) and dodecanoic acid ( $p=0.044$ ) were higher

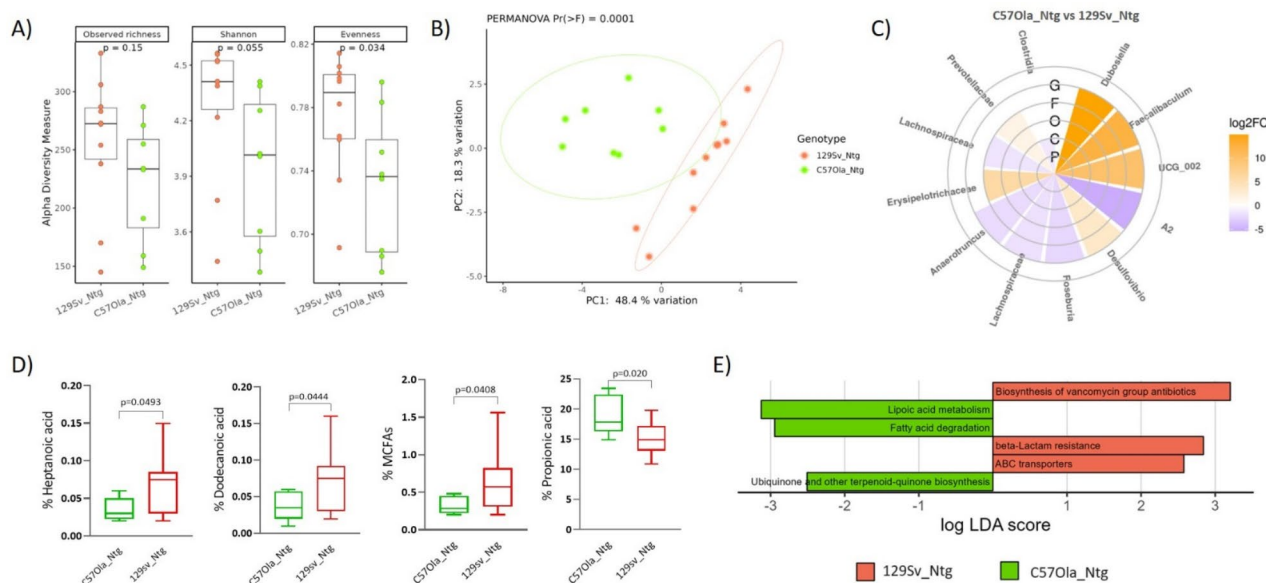


**Fig. 1** Comparative Analysis of Microbiota Composition and Metabolic Profiles in C57Ola<sub>Ntg</sub> and 129Sv<sub>Ntg</sub> Mice at 12 weeks' age. **(A)** Boxplots showcasing alpha diversity indices (Observed Richness, Shannon index, Evenness) in fecal samples. Statistical differences were evaluated using a paired Wilcoxon signed-rank test.  $P$ -values less than 0.05 were considered statistically significant. **(B)** Principal coordinates analysis (PCoA) according to the Hellinger distance computed on genera abundances. Results of the permutational multivariate analysis of variance (PERMANOVA) are also shown based on the first two coordinates. **(C)** Circular heatmap representing the differentially abundant taxa in C57Ola versus 129 Sv mice samples: concentric circles represent taxonomic ranks from phylum (P) to genus (G); yellow shades indicate positive  $\log_2FC$  values, whereas blue shades indicate negative  $\log_2FC$  values correlations; the intensity of colors is proportional to  $\log_2FC$  values. **(D)** Box plot reporting the statistically significant different free fatty acids among the two Ntg strains. **(E)** Computed Linear Discriminant Analysis (LDA) scores representing significantly differential KEGG Pathway Expression (LDA > 2.5) between 129Sv<sub>Ntg</sub> and C57Ola<sub>Ntg</sub> mice

whereas the level of propionic acid ( $p=0.020$ ) was lower in 129SvNtg mice than C57OlaNtg, (Fig. 1D). To corroborate these findings, functional prediction analysis using PICRUST revealed differential expression of several KEGG pathways between the two strains. Specifically, in C57OlaNtg mice, pathways related to fatty acid degradation, lipoic acid metabolism, ubiquinone and other terpenoid-quinone biosynthesis were more abundant. Conversely, in 129SvNtg mice, pathways associated with beta-lactam resistance, biosynthesis of vancomycin group antibiotics, and ABC transporters were more abundant (Fig. 1E).

Additionally, the temporal stability of the microbiota within each strain was examined over time. Supplementary figures depicting beta diversity at different ages for both C57OlaNtg and 129SvNtg mice illustrated that, in each strain, the microbiota composition remained relatively consistent as the mice aged (see Fig. 3 : Beta diversity at different ages for each strain, C57Ola Ntg, and 129 Sv Ntg).

### The presence of the human mutant SOD1G93A exerts an influence on gut microbial colonization

The presence of the SOD1 mutation induced significant shifts in GM colonization before the onset of the disease in both strains, with changes particularly evident in C57-G93A mice compared to their Ntg counterparts. At 12 weeks of age, C57Ola-G93A mice exhibited significant differences in microbiota composition compared to their Ntg littermates, as indicated by beta diversity analysis (PERMANOVA=0.0001) (Fig. 2A), while alpha diversity did not show significant differences (data not shown). Furthermore, DESeq analysis unveiled a significant decrease in specific microbial taxa in G93A mice, including Erysipelotrichaceae ( $\log_2FC=5.11$ ,  $\text{padj}<0.0001$ ) family, *NK3B31\_group* of Prevotellaceae ( $\log_2FC=8.89$ ,  $\text{padj}<0.0001$ ), *Dubosiella* ( $\log_2FC=11.97$ ,  $\text{padj}<0.0001$ ), and *Faecalibaculum* ( $\log_2FC=9.92$ ,  $\text{padj}<0.0001$ ) (Fig. 2B) genera. The fecal levels of total MCFA ( $p=0.005$ ), heptanoic acid ( $p=0.010$ ), dodecanoic acid ( $p=0.013$ ) and decanoic acid ( $p=0.039$ ) were higher in C57Ola\_G93A mice compared to C57OlaNtg, while the propionic acid was lower ( $p=0.0152$ ) (Fig. 2D). Interestingly, in C57Ola\_G93A, we observed negative correlations between the abundance of Erysipelotrichaceae

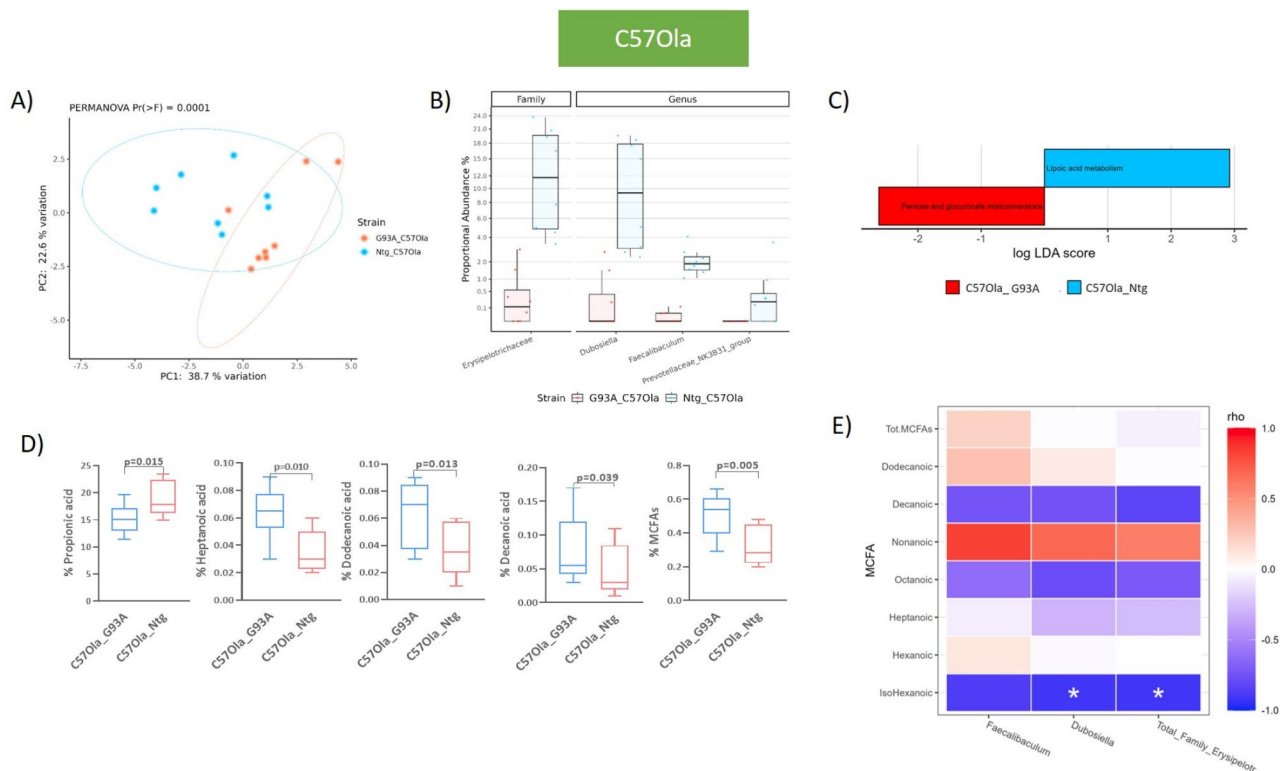


**Fig. 2** Microbiota Differences and Diversity Analyses in C57Ola Strain, Comparing Non-Transgenic (Ntg) and G93A Transgenic Mice at 12 Weeks of Age. **(A)** Principal coordinates analysis (PCoA) according to Hellinger distance computed on genera abundances. **(B)** Boxplots with the differentially abundant taxa. **(C)** Computed Linear Discriminant Analysis (LDA) scores representing significantly differential KEGG Pathway Expression (LDA > 2.5). **(D)** Boxplots of the significantly different free fatty acids. **(E)** Heatmap of correlations between MCFA levels and the relative abundance of the Erysipelotrichaceae, *Dubosiella* and *Faecalibaculum* taxa MCFA=medium chain fatty acids. \* $p$ -value < 0.05

( $Rho = -0.91$ ;  $padj = 0.04$ ) and *Dubosiella* ( $Rho = -0.91$ ;  $padj = 0.03$ ) and medium-chain fatty acids (MCFA), especially isohexanoic acid (Fig. 2E). PICRUST analysis revealed that lipoic acid metabolism was higher in Ntg compared to G93A mice (Fig. 2C).

Regarding the 129 Sv strain, subtle differences emerged when comparing the microbiome of  $SOD1^{G93A}$  mice to the Ntg littermates, with a minor yet significant separation observed in the PCoA plot (PERMANOVA = 0.0299) (Fig. 3A). Notably, only the genus *UCG-001* of Lachnospiraceae displayed a significant decrease in mice

with the G93A mutation ( $\log_2FC = 4.35$ ,  $padj < 0.0001$ ) (Fig. 3B) and no difference was observed in fecal SCFA and glycosaminoglycan degradation, as well as other glycan degradation pathways, in G93A 129 Sv mice compared to their non-transgenic counterparts (Fig. 3C).

**Distinct microbiota profiles in  $SOD1^{G93A}$  mutant mice strains: strain-specific profiles across disease progression**

The presence of the  $SOD1^{G93A}$  mutation does not induce a shared microbiota profile across the two strains. Both C57Ola\_G93A and 129Sv\_G93A mice exhibit distinct

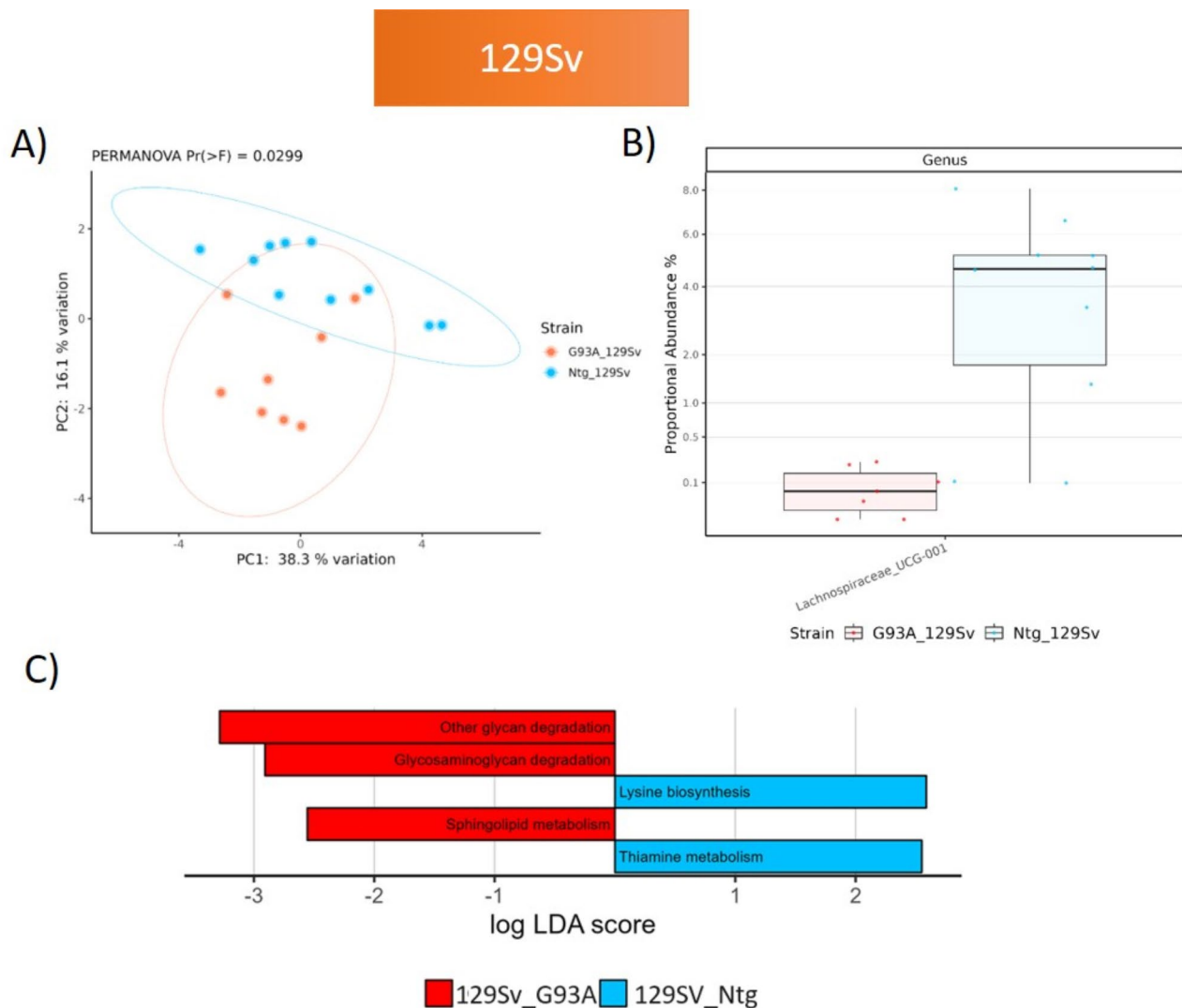


**Fig. 3** Microbiota Differences and Diversity Analyses in 129 Sv Strain, Comparing Non-Transgenic (Ntg) and G93A Transgenic Mice at 12 Weeks of Age. **(A)** Principal coordinates analysis (PCoA) according to Hellinger distance computed on genera abundances. **(B)** Boxplots with the differentially abundant taxa. **(C)** Computed Linear Discriminant Analysis (LDA) scores representing significantly differential KEGG Pathway Expression (LDA > 2.5)

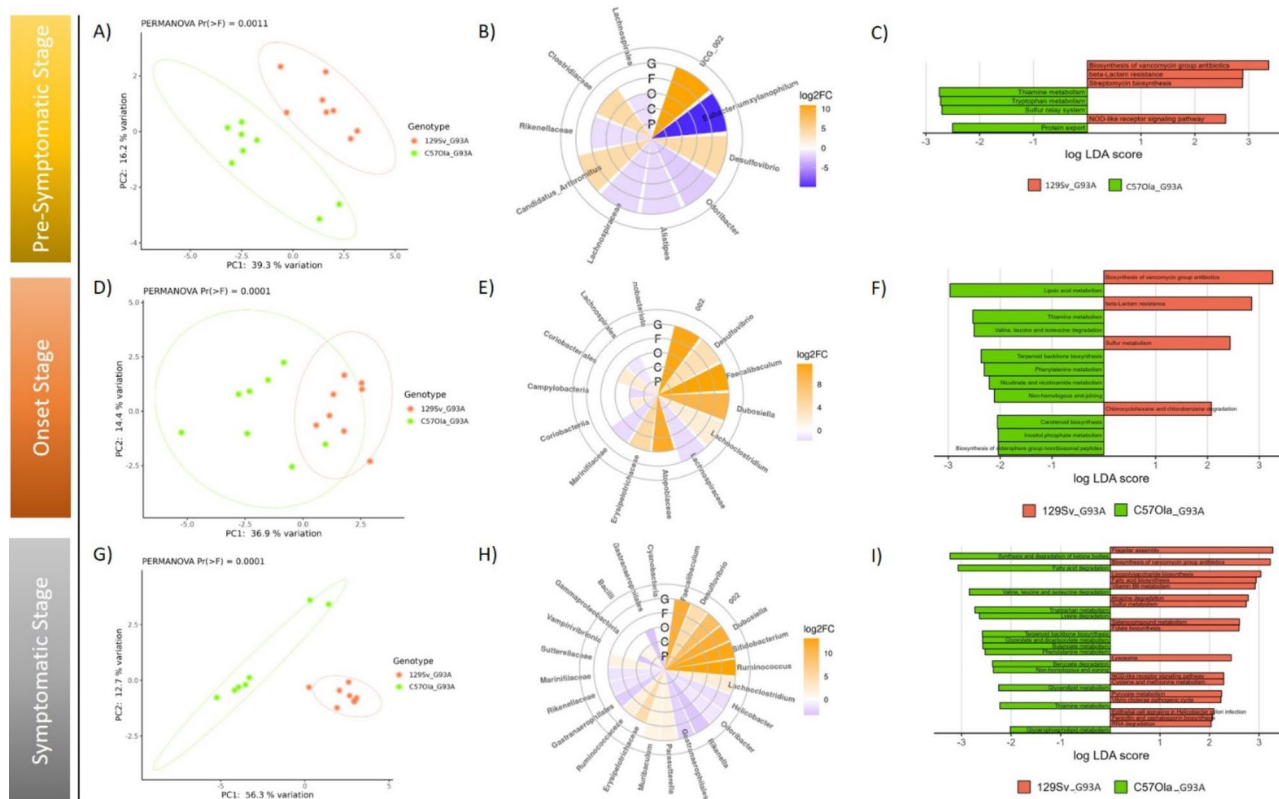


**Fig. 4** Temporal analysis of microbiota between C570la\_G93A and 129Sv\_G93A mice. Beta diversity, as well as DESeq2 and PICRUST2 analysis, were conducted at the pre-symptomatic stage (PS) in panels **A, B,** and **C**; at disease onset (OS) in panels **D, E,** and **F**; and during the symptomatic stage (SY) in panels **G, H,** and **I**. LDA=linear discriminant analysis

microbial profiles, characterized by significant beta diversity (PERMANOVA=0.0009), with numerous bacterial taxa showing differential expression between the two strains, across the disease course (refer to Fig. 4). Notably, at a pre-symptomatic stage, some of the differences observed among the non-transgenic strains are present also among SOD1<sup>G93A</sup> mice, with the *unidentified genus* of Lachnospiraceae clade remaining higher in 129 Sv compared to C570la, and the *Coriobacteriaceae\_UCG-002* genus remaining more abundant in C570la. Conversely, members of the Erysipelotrichaceae family (*Dubosiella* and *Faecalibaculum*) and fatty acids levels no longer exhibit differential abundance among the SOD1<sup>G93A</sup> mutated strains. Additionally, it is noteworthy that no pathways related to lipid metabolism exhibited differential abundance between 129Sv\_G93A and C570la\_G93A mice in the functional prediction analysis (Fig. 4C).

As disease onset and symptomatic stages progress, many differences persist in the microbiota composition between the two strains (Fig. 4). Particularly noteworthy is the resurgence of Erysipelotrichaceae in C570la\_G93A compared to 129Sv\_G93A, alongside alterations in lipid metabolism. Remarkably, at the symptomatic

stage, C570la mice exhibit an upregulation in fatty acid degradation (LDA=3;  $p=0.034$ ) and an increase in the synthesis and degradation of ketone bodies (LDA=3.2;  $p=0.002$ ), while 129 Sv mice show a rise in fatty acid biosynthesis (LDA=2.9;  $p=0.004$ ) (Fig. 4I).

Finally, the temporal microbiota stability was assessed over time and, in each SOD1<sup>G93A</sup> strain, the microbiota composition remained relatively consistent throughout the disease stages (see Figure S3).

#### Systemic immunity and inflammatory response

Similar to the microbiota, the systemic immune-phenotype profile was significantly different between the two Ntg mouse strains at 12 weeks' age. Notably, in the blood, proinflammatory monocytes (Ly6C+) were significantly higher in C570la\_Ntg versus 129Sv\_Ntg mice. Conversely, the patrolling monocytes (Ly6C-) were higher in 129Sv\_Ntg compared to C570la strain (Fig. 5A). For the SOD1<sup>G93A</sup> mice, only the 129 Sv strain showed a difference compared to their respective NTG mice, with an increase in proinflammatory monocytes and a decrease in patrolling monocytes at the presymptomatic stage (Fig. 5A). No differences were observed in the C570la\_G93A mice compared to their respective NTG mice for



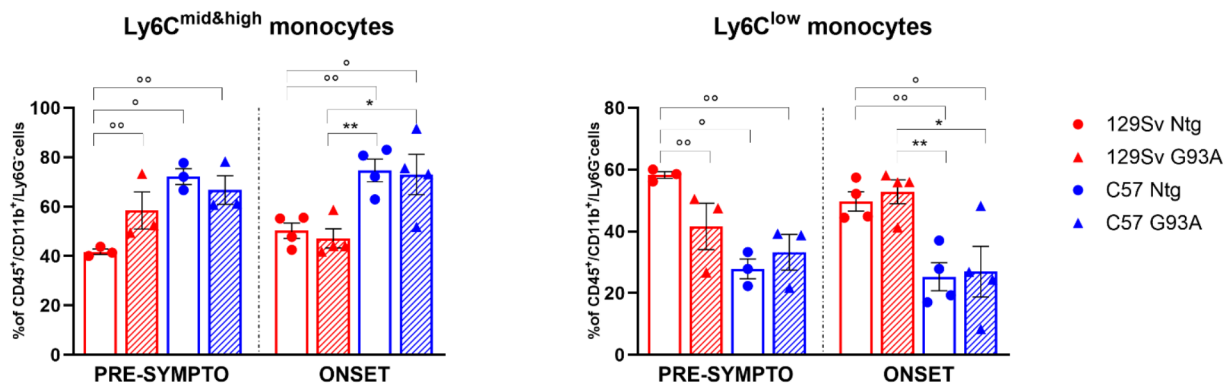


**Fig. 5** Analysis of circulating monocyte populations across different time points and mouse strains. Proinflammatory monocytes are identified as CD45+CD11b+Ly6C+ cells, while patrolling monocytes are defined as CD45+CD11b+Ly6C- cells. Data are expressed as mean ± SEM of *n* = 3–4 mice per experimental group. \**p* < 0.05, °*p* < 0.01 (129 Sv Ntg Vs 129 Sv G93A, C57 Ntg and C57 G93A); \**p* < 0.05, \*\**p* < 0.01 (129 Sv G93A Vs 129 Sv Ntg, C57 Ntg and C57 G93A) by two-way-ANOVA with Fisher post-analysis

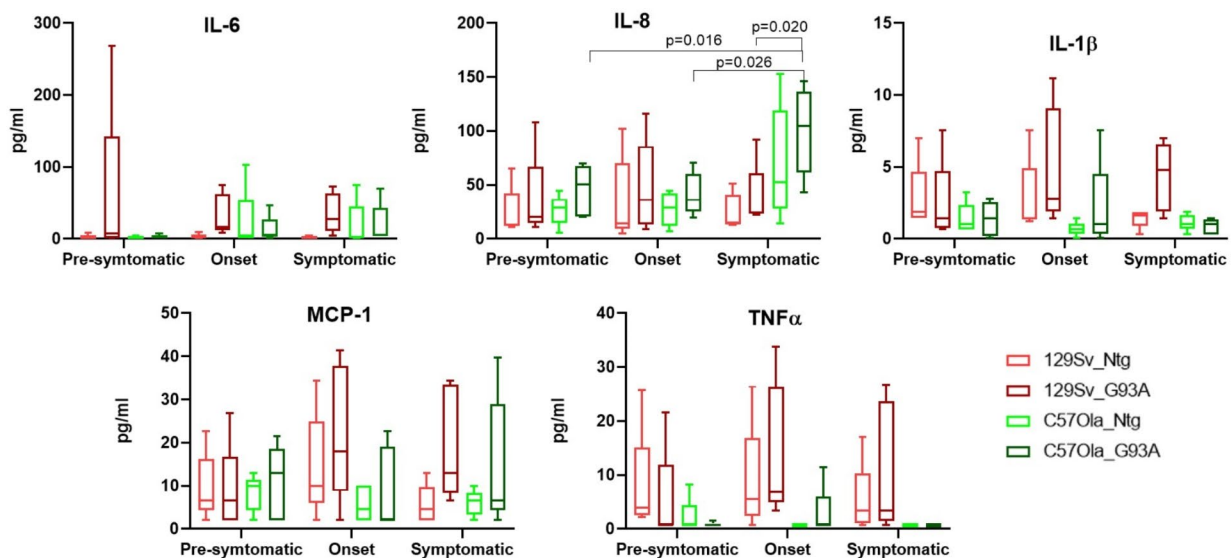


**Fig. 6** Serum cytokine levels across different time points and mouse strains. Boxplot showing the serum cytokines levels. Comparison between time points and strains were performed by two-way ANOVA using Tukey’s multiple comparisons post-test. \* adjusted *p* value < 0.05

either monocyte population. At the onset age, significant differences in both monocyte populations were still present between the NTG of the two mouse strains. However, the difference between the 129Sv\_G93A mice and their respective NTG mice was not maintained (Fig. 5B). Unfortunately, analysis at the symptomatic stage was hindered by a scarcity of available blood samples from the mice.

No statistically significant differences in peripheral blood cytokine levels were observed between SOD1<sup>G93A</sup> and Ntg littermates across all examined time points. Also, the cytokine levels in both SOD1<sup>G93A</sup> mice demonstrated minimal variation throughout disease progression, except

for KC/IL-8 that exhibited an increase during the symptomatic stage in C57Ola\_G93A mice compared to the PS (*p* = 0.016) and OS (*p* = 0.026) stages (see Fig. 6). When comparing SOD1<sup>G93A</sup> mice across strains, significant differences emerged at the symptomatic stage. Specifically, KC levels were significantly higher in C57Ola\_G93A compared to 129Sv\_G93A, indicating a distinct response (*p* = 0.020). Additionally, a discernible, although not statistically significant trend was observed for TNFα and IL-1β, which appeared higher in 129Sv\_G93A than C57Ola\_G93A peripheral blood at onset and symptomatic stages. This suggests a potential strain-specific

variation in the immune response, although the significance was not retained after post-test adjustment of  $p$  values.

## Discussion

Recent research highlights the complex relationship between gut microbiota and ALS progression, suggesting that dysbiosis and altered metabolites' profiles may contribute to disease progression through mechanisms involving the brain-gut-microbiota axis [7, 15, 27]. Despite extensive studies, the right causative factors remain unclear; however, understanding these dynamics may be critical for developing effective diagnostic and therapeutic strategies for ALS. Our investigation delved into the intricate interplay among genetic factors, GM composition, metabolism, and immune response within ALS mouse models. Specifically, we analyzed two distinct SOD1<sup>G93A</sup> mice strains, along with their Ntg littermates: 129Sv\_G93A, characterized by rapid disease progression and C57Ola\_G93A, exhibiting a slower course. This contrast highlights the substantial impact of genetic background on ALS trajectory.

### The contribution of the genetic background to the microbiota and inflammation

First, we observed strain-specific nuances in microbiota composition and fecal metabolites between C57Ola and 129 Sv strains, with taxonomic analysis revealing a diverse microbial landscape dominated by *Firmicutes*, *Bacteroidota*, and *Campilobacterota* [31, 49]. Previous studies suggest that genetic background significantly influences GM composition [56]. For example, BALB/c mice exhibit greater microbial diversity and distinct compositional variations compared to other strains [24, 28, 36].

The 129 Sv strain displayed a more consistent microbial profile, characterized by an increase in butyrate-producing taxa from the Clostridia and Lachnospiraceae families, and a reduction Erysipelotrichaceae genera (*Dubosiella* and *Faecalibaculum*) and the UCG-002 genus of Coriobacteriaceae family. Differences in fecal fatty acid levels was observed, with SCFA and MCFA playing essential roles as both energy-supplying metabolites and signalling molecules involved in regulating lipid metabolism. Abnormal levels over time can contribute to inflammation and insulin resistance, potentially leading to several diseases, including diabetes, neurodegenerative diseases, and cancer [19, 34]. MCFA, such as capric acid and lauric acid, are primarily obtained from medium-chain triglycerides in dietary sources like milk and plant oils, but can also be produced by GM [59, 60]. For instance, yeast strains, like *Saccharomyces cerevisiae*, produce caprylate (C8) via EHT1 and EEB1 genes, which facilitate medium-chain fatty acid synthesis [60]. Recent

studies show that GM can rapidly metabolize MCFA to produce energy in the colon, with Erysipelotrichaceae, Peptococcaceae, and other taxa positively correlating with cecal MCFA concentrations [30]. MCFA are readily absorbed and metabolized in liver mitochondria, producing ketone bodies that can enhance cerebral energy metabolism during low glucose availability [13, 26, 55]. Daily consumption of MCFA, such as coconut oil or triglycerides, has been linked to neuroprotection and cognitive benefits in ALS models [21, 55]. SCFA, produced by GM through the fermentation of dietary fibers, modulate immune responses via G protein-coupled receptors (GPCRs) such as GPR41 and GPR43, improving intestinal barrier integrity and promoting anti-inflammatory response [58]. Additionally, SCFAs act as histone deacetylase (HDAC) inhibitors, modulating gene expression to support barrier functions and immune cell activation [46]. Conversely, MCFAs act primarily through GPR84, triggering proinflammatory responses, including chemotaxis of immune cells, and increased production of cytokines like IL-8 and TNF $\alpha$  in response to lipopolysaccharide (LPS) stimulation [65].

Notably, 129Sv\_Ntg mice displayed higher total MCFA levels, especially heptanoic acid and dodecanoic acid, and a reduction in propionic acid compared to same-age C57Ola mice. This discrepancy may stem from inherent genetic variability influencing fatty acid metabolism, as 129Sv mice have a higher metabolic rate and a fat oxidation capacity [4]. These metabolic differences likely contribute to variations in substrate utilization patterns, impacting the processing and excretion of MCFA. Furthermore, GM plays a crucial role in modulating dietary component metabolism. It is plausible that the GM of 129 Sv mice possesses specific enzymatic capabilities or preferential pathways for metabolizing MCFA, leading to alterations in fecal fatty acid profiles. Conversely, differences in microbial composition and functionality in C57Ola mice may result in distinct metabolic outcomes for these fatty acids. Functional prediction revealed that C57Ola mice have higher lipid metabolism potential possibly linked to the abundance of Erysipelotrichaceae, which correlates with MCFA levels [38].

The divergent GM compositions may also contribute to differential immune responses; for instance, lower *Faecalibaculum* levels in C57Ola mice corresponded with a higher proportion of proinflammatory monocytes compared to 129 Sv mice [71].

Given the observed differences in cytokine levels and monocytic profiles between 129 Sv and C57OlaNtg mice, we propose a hypothesis regarding the underlying metabolic and immune mechanisms. The higher fecal levels of MCFA in 129 Sv mice might indicate lower systemic levels of these fatty acids, as MCFA are rapidly absorbed and metabolized. This could lead to reduced availability

of MCFA in the bloodstream, which may favour a less proinflammatory monocytic profile. Conversely, the lower fecal levels of SCFA in 129 Sv mice might correspond to higher systemic concentrations, as SCFA are efficiently absorbed and promote the patrolling phenotype of monocytes, exerting anti-inflammatory effects. Alternatively, differential expression of fatty acid receptors could explain these observations. SCFAs and MCFAs mediate their effects through receptors such as GPR41, GPR43, and GPR84. Higher receptor expression in 129 Sv mice might enhance the anti-inflammatory signaling of SCFA, even at similar systemic concentrations. In contrast, elevated GPR84 expression could influence the proinflammatory effects of MCFAs, accounting for the higher proinflammatory monocyte levels in C57OlaNtg mice. The elevated levels of proinflammatory cytokines (e.g., TNF- $\alpha$  and MCP-1) in 129 Sv Ntg mice, despite a higher proportion of patrolling monocytes, may indicate a compensatory immune response attempting to counterbalance the systemic inflammatory environment. In contrast, C57BL/6 Ntg mice, with lower fecal levels of MCFA, might retain more of these fatty acids systemically, contributing to higher levels of proinflammatory monocytes and potentially a more direct proinflammatory state. Additionally, higher fecal SCFA levels in C57Ola mice could indicate lower systemic availability, diminishing anti-inflammatory effects. Therefore, the differential expression of fatty acid receptors warrants further investigation.

These findings suggest a complex interplay between gut-derived metabolites and systemic immune responses, where the balance of MCFA and SCFA may significantly influence the inflammatory status and the phenotypic distribution of monocytes. Besides, we demonstrated that genetic background may influence differences in energetic metabolism and immune response modulation capacity of the GM, potentially contributing to variable susceptibility to disease. Further studies are needed to explore the systemic levels of these fatty acids and their mechanisms in modulating immune cell function in different genetic backgrounds, potentially leading to novel therapeutic strategies for managing inflammation in ALS.

#### The contribution of SOD1<sup>G93A</sup> to the microbiota and inflammation

The SOD1<sup>G93A</sup> mutation influenced GM colonization in both strains, albeit to varying extents. In a pre-symptomatic stage, C57Ola\_G93A mice exhibited a significant microbiota shift compared to their Ntg littermates, whereas the 129 Sv G93A strain showed subtle changes, suggesting a more stable baseline microbiota profile less susceptible to mutation-induced perturbations. Interestingly, in C57Ola\_G93A mice, specific taxa, such as Erysipelotrichaceae, Prevotellaceae NK3B31\_group,

*Dubosiella*, and *Faecalibaculum* decreased, while total MCFA, heptanoic acid, dodecanoic acid, and decanoic acid levels increased, alongside reduced propionic acid. The mutation-induced shift led C57Ola\_G93A mice to acquire similarities with 129 Sv but in some taxa and metabolite levels, such as Clostridia, Lachnospiraceae, Erysipelotrichaceae, *Dubosiella*, and *Faecalibaculum* as well as SCFA and MCFA levels. This suggests that the SOD1<sup>G93A</sup> mutation in C57Ola mice may induce microbiota changes resembling those of 129 Sv strain, potentially contributing to disease pathogenesis or progression. Erysipelotrichaceae and Coriobacteriaceae have been linked to host lipid metabolism and dyslipidemic phenotypes [16, 43, 44, 70]. While Clostridia and Lachnospiraceae are significant producers of beneficial SCFA, Lachnospiraceae has also been associated with glucose and/or lipid metabolism disturbances, indicating potential metabolic dysregulation [14, 39, 62]. Furthermore, Lachnospiraceae *genus bacterium A4* has been associated with disease progression in SOD1<sup>G93A</sup> ALS mice [72], suggesting a complex role of this taxon in both host health and disease [67].

The elevation of MCFA levels and reduction of SCFA in C57Ola\_G93A mice may mirror a connection between mutant SOD1 expression and fatty acid metabolism, as MCFA are associated with inflammation and higher levels in ALS patients [54]. The lower propionic acid level in both 129Sv\_Ntg mice and C57Ola\_G93A could indicate altered anti-inflammatory pathways. Notably, propionic acid is known to reduce inflammatory cytokines (TNF- $\alpha$  and IP-10) and promote metabolic health [1–3, 33].

Additionally, C57Ola\_G93A strain demonstrated distinct immune responses compared to the 129Sv\_G93A, with increased Erysipelotrichaceae, *Dubosiella*, and *Faecalibaculum* levels observed at disease onset and late stages. Strain-specific increases in cytokine KC/IL-8 during the symptomatic stage further reflect the immune profile changes in these mutated strains. Although we could not measure fecal fatty acid levels during the onset and symptomatic stages due to material constraints, functional pathway prediction estimated significant increases in lipoic acid metabolism and fatty acid degradation in C57Ola\_G93A mice compared to 129Sv\_G93A. The predicted upregulation of fatty acid degradation and ketone body metabolism in C57Ola\_G93A mice may suggest an enhanced utilization of fatty acids for energy production, possibly as a compensatory mechanism for the impaired energy metabolism associated with ALS progression, which is not observed in 129Sv\_G93A microbiota.

Lastly, our assessment of temporal changes within the same strains documented no significant shifts in alpha or beta diversity, suggesting that GM composition remained relatively stable throughout disease progression. This contrasts with previous studies reporting microbiota

changes over time in both ALS patient [20] and animal models [27]. Differences in study design, confounding variables (e.g., diet, environment), and the use of distinct strains likely account for these disparities. However, our findings do not exclude potential subtle alterations in specific microbial genera or functional properties. A more comprehensive approach, such as shotgun metagenomic sequencing, could reveal functionally relevant changes that 16 S rRNA sequencing may have missed.

## Conclusions

Overall, these findings suggest that genetic background may influence differences in energetic metabolism and immune response modulation capacity of the GM in the two strains, potentially contributing to variable susceptibility to disease. Since the housing facility has been reported to significantly impact the mouse survival and microbiota [11, 27], the advantage of this study is that both fast and slow disease-progressing mouse cohorts are housed in the same facility and receive the same diet, so the potential diversity of their microbiota and immune/inflammatory system in relation to their survival may be due exclusively to the different genetic background.

We acknowledge that mice were analyzed at different time points (16 or 22 weeks) due to variations in disease progression, which may introduce biological variability. While we focused on the pre-symptomatic phase (12 weeks) for microbiota and fatty acid comparisons, immune responses were assessed at both onset and symptomatic stages. Age-related factors may have influenced immune outcomes, which should be considered when interpreting these results.

The functional and compositional variations in the GM, particularly in MCFA metabolism and specific bacterial taxa, such as Erysipelotrichaceae, may show predisposition to ALS. Further research is needed to clarify their role in disease progression.

Surely, the study has some limitations; firstly, we primarily relied on fecal samples which may not fully capture microbial diversity and functionality throughout the gastrointestinal tract. Additionally, we did not assess circulating free fatty acids, and our taxonomic resolution was limited to the genus level. Future studies employing metagenomic or metatranscriptomic approaches could provide more detailed taxonomic information, enhancing our understanding of GM composition in ALS.

Future mechanistic studies, including fecal microbiota transplantation (FMT) experiments, targeted interventions or genetic manipulations, could elucidate the causal relationships between genetic background, GM, and ALS pathology. In detail, FMT will allow for a more rigorous assessment of the causal GM effects on ALS progression. Additionally, research focused on elucidating the metabolic pathways and enzymatic mechanisms involved

in medium-chain fatty acid metabolism in ALS models could provide valuable insights into their role in disease progression.

## Abbreviations

ALS	Amyotrophic lateral sclerosis
SOD	Superoxide dismutase
GM	Gut microbiota
FFA	Free fatty acids
SCFA	Short chain fatty acids
MCFA	Medium chain fatty acids

## Supplementary Information

The online version contains supplementary material available at <https://doi.org/10.1186/s40478-024-01877-x>.

Supplementary Material 1

## Acknowledgements

Not applicable.

## Author contributions

A.A., E.N., G.N., C.B.: Conceptualization and Methodology; E.N., G.N., S.B., M.C.T., P.F., C.M.: Investigation; L.D.G., M.C.T., S.B., C.N., E.N.: Formal Analysis; A.A., G.N., C.B.: Resources; E.N., M.C.T., L.D.G.: Writing- Original draft preparation; L.D.G., E.N., M.C.T.: Visualization; C.B., A.A., G.B., M.R.: Supervision; E.N., C.N., G.N., C.B., A.A.: Writing- Reviewing and Editing.

## Funding

C.N. is supported by Fondazione Beppe and Nuccy Angiolini Onlus. M.C.T. is supported by Ministry of Health, Ricerca Finalizzata- Starting Grant (SG-2019-12371083). A.A. is supported by #NEXTGENERATIONEU (NGEU) and funded by the Ministry of University and Research (MUR), National Recovery and Resilience Plan (NRRP), project MNESYS (PE0000006) – A Multiscale integrated approach to the study of the nervous system in health and disease (DR. 1553 11.10.2022).

## Data availability

The datasets generated in this study are publicly available in NCBI Gene Expression Omnibus (GEO) repository at <https://www.ncbi.nlm.nih.gov/geo/query/acc.cgi?acc=GSE278875>. The data that support the findings of this study are available at [https://github.com/LeandroD94/Papers/tree/main/2024\\_SL\\_A\\_mice\\_Fast129Sv\\_SlowC57\\_G93A](https://github.com/LeandroD94/Papers/tree/main/2024_SL_A_mice_Fast129Sv_SlowC57_G93A). Data not included in the repository are available upon request.

## Declarations

### Ethics approval and consent to participate

Procedures involving animals and their care were conducted according to the Mario Negri institutional guidelines, which comply with national (D.L. no. 116, G.U. suppl. 40, Feb.18, 1992, Circular No.8, G.U., 14 July 1994) and international policies (EEC Council Directive 86/609, OJ L 358, 1 Dec.12, 1987; NIH Guide for the Care and use of Laboratory Animals, U.S. National Research Council, 1996). All experiments and protocols were examined by the Institutional Ethical Committee and authorized by the Italian Ministry of Health.

### Consent for publication

not applicable.

### Competing interests

The authors declare no competing interests.

### Author details

<sup>1</sup>Department of Experimental and Clinical Medicine, University of Florence, Largo Brambilla 3, Florence 50134, Italy

<sup>2</sup>Department of Experimental and Clinical Biomedical Sciences "Mario Serio", University of Florence, Viale Morgagni 50, Florence 50134, Italy

<sup>3</sup>Laboratory of Molecular Neurobiology and Preclinical Therapy, Department of Neuroscience, Istituto di Ricerche Farmacologiche Mario Negri IRCCS, Via Mario Negri 2, Milano 20156, Italy

<sup>4</sup>Unit of Immunopharmacology, Department of Experimental Oncology, Istituto di Ricerche Farmacologiche Mario Negri IRCCS, Via Mario Negri 2, Milano 20156, Italy

<sup>5</sup>Department of Neurosciences, Psychology, Drug Research and Child Health Section of Pharmaceutical and Nutraceutical Sciences, University of Florence, Viale Pieraccini 6, Florence 50139, Italy

Received: 1 August 2024 / Accepted: 16 October 2024

Published online: 06 November 2024

## References

- Al-Lahham S, Rezaee F (2019) Propionic acid counteracts the inflammation of human subcutaneous adipose tissue: a new avenue for drug development. *Daru: J Fac Pharm Tehran Univ Med Sci* 27:645–652. <https://doi.org/10.1007/s40199-019-00294-z>
- Al-Lahham S, Roelofsen H, Rezaee F, Weening D, Hoek A, Vonk R, Venema K (2012) Propionic acid affects immune status and metabolism in adipose tissue from overweight subjects. *Eur J Clin Invest* 42:357–364. <https://doi.org/10.1111/j.1365-2362.2011.02590.x>
- Al-Lahham Sa, Roelofsen H, Rezaee F, Weening D, Hoek A, Vonk R, Venema K (2012) Propionic acid affects immune status and metabolism in adipose tissue from overweight subjects. 42:357–364. <https://doi.org/10.1111/j.1365-2362.2011.02590.x>
- Almind K, Kahn CR (2004) Genetic determinants of Energy expenditure and Insulin Resistance in Diet-Induced obesity in mice. *Diabetes* 53:3274–3285. <https://doi.org/10.2337/diabetes.53.12.3274>. %J Diabetes
- Beers DR, Appel SH (2019) Immune dysregulation in amyotrophic lateral sclerosis: mechanisms and emerging therapies. *Lancet Neurol* 18:211–220. [https://doi.org/10.1016/s1474-4422\(18\)30394-6](https://doi.org/10.1016/s1474-4422(18)30394-6)
- Bendotti C, Carri MT (2004) Lessons from models of SOD1-linked familial ALS. *Trends Mol Med* 10:393–400. <https://doi.org/10.1016/j.molmed.2004.06.009>
- Blacher E, Bashiardes S, Shapiro H, Rothschild D, Mor U, Dori-Bachash M, Kleimayer C, Moresi C, Harnik Y, Zur M et al (2019) Potential roles of gut microbiome and metabolites in modulating ALS in mice. *Nature* 572: 474–480 <https://doi.org/10.1038/s41586-019-1443-5>
- Blasco H, Lanznaster D, Veyrat-Durebex C, Hergesheimer R, Vourch P, Maillet F, Andres CR, Pradat PF, Corcia P (2020) Understanding and managing metabolic dysfunction in amyotrophic lateral sclerosis. *Expert Rev Neurother* 20:907–919. <https://doi.org/10.1080/14737175.2020.1788389>
- Bokulich NA, Subramanian S, Faith JJ, Gevers D, Gordon JI, Knight R, Mills DA, Caporaso JG (2013) Quality-filtering vastly improves diversity estimates from Illumina amplicon sequencing. *Nat Methods* 10:57–59. <https://doi.org/10.1038/nmeth.2276>
- Bouteloup C, Desport JC, Clavelou P, Guy N, Derumeaux-Burel H, Ferrier A, Couratier P (2009) Hypermetabolism in ALS patients: an early and persistent phenomenon. *J Neurol* 256:1236–1242. <https://doi.org/10.1007/s00415-009-5100-z>
- Burberry A, Wells MF, Limone F, Couto A, Smith KS, Keaney J, Gillet G, van Gastel N, Wang JY, Pietilainen O et al (2020) C9orf72 suppresses systemic and neural inflammation induced by gut bacteria. *Nature* 582:89–94. <https://doi.org/10.1038/s41586-020-2288-7>
- Cao Q, Sun X, Rajesh K, Chalasani N, Gelow K, Katz B, Shah VH, Sanyal AJ, Smirnova E (2020) Effects of Rare Microbiome Taxa filtering on statistical analysis. *Front Microbiol* 11:607325. <https://doi.org/10.3389/fmicb.2020.607325>
- Chatterjee P, Fernando M, Fernando B, Dias CB, Shah T, Silva R, Williams S, Pedrini S, Hillebrandt H, Goozee K et al (2020) Potential of coconut oil and medium chain triglycerides in the prevention and treatment of Alzheimer's disease. *Mech Ageing Dev* 186:111209. <https://doi.org/10.1016/j.mad.2020.111209>
- Chávez-Carbajal A, Nirmalkar K, Pérez-Lizaur A, Hernández-Quiroz F, Ramírez-Del-Alto S, García-Mena J, Hernández-Guerrero C (2019) Gut microbiota and predicted metabolic pathways in a sample of Mexican Women affected by obesity and obesity plus metabolic syndrome. *Int J Mol Sci* 20. <https://doi.org/10.3390/ijms20020438>
- Chen S, Cai X, Lao L, Wang Y, Su H, Sun H (2024) Brain-gut-microbiota Axis in Amyotrophic lateral sclerosis: a historical overview and future directions. *Ageing Disease* 15:74–95. <https://doi.org/10.14336/ad.2023.0524>
- Claus SP, Ellero SL, Berger B, Krause L, Bruttin A, Molina J, Paris A, Want EJ, Waziers Id, Cloarec O et al (2011) Colonization-Induced Host-Gut Microbial Metabolic Interaction. 2: <https://doi.org/10.1128/mbio.00271-10> Doi doi:10.1128/mbio.00271-10
- Coque E, Salsac C, Espinosa-Carrasco G, Varga B, Degauque N, Cadoux M, Crabé R, Virenque A, Soulard C, Fierle JK et al (2019) Cytotoxic CD8(+) T lymphocytes expressing ALS-causing SOD1 mutant selectively trigger death of spinal motoneurons. *Proc Natl Acad Sci USA* 116:2312–2317. <https://doi.org/10.1073/pnas.1815961116>
- De Marchi F, Munitic I, Amedei A, Berry JD, Feldman EL, Aronica E, Nardo G, Van Weehaeghe D, Niccolai E, Prtenjaca Net et al (2021) Interplay between immunity and amyotrophic lateral sclerosis: clinical impact. *Neurosci Biobehav Rev* 127:958–978. <https://doi.org/10.1016/j.neubiorev.2021.06.027>
- den Besten G, van Eunen K, Groen AK, Venema K, Reijngoud D-J, Bakker BM (2013) The role of short-chain fatty acids in the interplay between diet, gut microbiota, and host energy metabolism. *J Lipid Res* 54:2325–2340. <https://doi.org/10.1194/jlr.R036012>
- Di Gioia D, Bozzi Cionci N, Baffoni L, Amoroso A, Pane M, Mogna L, Gaggia F, Lucenti MA, Bersano E, Cantello Ret et al (2020) A prospective longitudinal study on the microbiota composition in amyotrophic lateral sclerosis. *BMC Med* 18:153. <https://doi.org/10.1186/s12916-020-01607-9>
- Dunn E, Steinert JR, Stone A, Sahota V, Williams RSB, Snowden S, Augustin H (2023) Medium-chain fatty acids rescue motor function and Neuromuscular Junction Degeneration in a Drosophila model of amyotrophic lateral sclerosis. *Cells* 12. <https://doi.org/10.3390/cells12172163>
- Dupuis L, Corcia P, Fergani A, Gonzalez De Aguilar JL, Bonnefont-Rousselot D, Bittar R, Seilhean D, Hauw JJ, Lacomblez L, Loeffler JP et al (2008) Dyslipidemia is a protective factor in amyotrophic lateral sclerosis. *Neurology* 70: 1004–1009 <https://doi.org/10.1212/01.wnl.0000285080.70324.27>
- Echaniz-Laguna A, Zoll J, Ribera F, Tranchant C, Warter JM, Lonsdorfer J, Lampert E (2002) Mitochondrial respiratory chain function in skeletal muscle of ALS patients. *Ann Neurol* 52:623–627. <https://doi.org/10.1002/ana.10357>
- Elderman H, Hugenholtz F, Belzer C, Boekschoten M, van Beek A, de Haan B, Savelkoul H, de Vos P, Faas M (2018) Sex and strain dependent differences in mucosal immunology and microbiota composition in mice. *Biology sex Differences* 9:26. <https://doi.org/10.1186/s13293-018-0186-6>
- Feldman EL, Goutman SA, Petri S, Mazzini L, Savelieff MG, Shaw PJ, Sobue G (2022) Amyotrophic lateral sclerosis. *Lancet (London England)* 400:1363–1380. [https://doi.org/10.1016/s0140-6736\(22\)01272-7](https://doi.org/10.1016/s0140-6736(22)01272-7)
- Fernando WM, Martins IJ, Goozee KG, Brennan CS, Jayasena V, Martins RN (2015) The role of dietary coconut for the prevention and treatment of Alzheimer's disease: potential mechanisms of action. *Br J Nutr* 114:1–14. <https://doi.org/10.1017/s0007114515001452>
- Figueroa-Romero C, Guo K, Murdock BJ, Paez-Colasante X, Bassis CM, Mikhail KA, Pawlowski KD, Evans MC, Taubman GF, McDermott A et al (2019) Temporal evolution of the microbiome, immune system and epigenome with disease progression in ALS mice. *Dis Models Mech* 13. <https://doi.org/10.1242/dmm.041947>
- Fransen F, Zagato E, Mazzini E, Fosso B, Manzari C, El Aidy S, Chiavelli A, D'Erchia AM, Sethi MK, Pabst O et al (2015) BALB/c and C57BL/6 mice Differ in Polyreactive IgA abundance, which impacts the generation of Antigen-Specific IgA and Microbiota Diversity. *Immunity* 43:527–540. <https://doi.org/10.1016/j.immuni.2015.08.011>
- Goutman SA, Hardiman O, Al-Chalabi A, Chió A, Savelieff MG, Kiernan MC, Feldman EL (2022) Emerging insights into the complex genetics and pathophysiology of amyotrophic lateral sclerosis. *Lancet Neurol* 21:465–479. [https://doi.org/10.1016/s1474-4422\(21\)00414-2](https://doi.org/10.1016/s1474-4422(21)00414-2)
- Gregor A, Auernigg-Haselmaier S, Trajanoski S, König J, Duszka K (2021) Colonic medium-chain fatty acids act as a Source of Energy and for Colon Maintenance but are not utilized to Acylate Ghrelin. *Nutrients* 13. <https://doi.org/10.3390/nu13113807>
- Guo J, Song C, Liu Y, Wu X, Dong W, Zhu H, Xiang Z, Qin C (2022) Characteristics of gut microbiota in representative mice strains: implications for biological research. *Anim Models Experimental Med* 5:337–349. <https://doi.org/10.1002/ame2.12257>
- Guo K, Figueroa-Romero C, Noureldein MH, Murdock BJ, Savelieff MG, Hur J, Goutman SA, Feldman EL (2023) Gut microbiome correlates with plasma lipids in amyotrophic lateral sclerosis. *Brain*. <https://doi.org/10.1093/brain/awad306>
- Heimann E, Nyman M, Degerman E (2015) Propionic acid and butyric acid inhibit lipolysis and de novo lipogenesis and increase insulin-stimulated

- glucose uptake in primary rat adipocytes. *Adipocyte* 4:81–88. <https://doi.org/10.4161/21623945.2014.960694>
34. Huang L, Gao L, Chen C (2021) Role of medium-chain fatty acids in healthy metabolism: a clinical perspective. *Trends Endocrinol Metab* 32:351–366. <https://doi.org/10.1016/j.tem.2021.03.002>
  35. Kato S (2008) Amyotrophic lateral sclerosis models and human neuropathology: similarities and differences. *Acta Neuropathol* 115:97–114. <https://doi.org/10.1007/s00401-007-0308-4>
  36. Korach-Rechtman H, Freilich S, Gerassy-Vainberg S, Buhnik-Rosenblau K, Danin-Poleg Y, Bar H, Kashi Y (2019) Murine genetic background has a stronger impact on the composition of the gut microbiota than maternal inoculation or exposure to unlike exogenous microbiota. *Appl Environ Microbiol* 85. <https://doi.org/10.1128/aem.00826-19>
  37. Lee CH, Olson P, Evans RM (2003) Minireview: lipid metabolism, metabolic diseases, and peroxisome proliferator-activated receptors. *Endocrinology* 144:2201–2207 Doi 10.1210/en.2003–0288
  38. Li W, Lan T, Ding Q, Ren Z, Tang Z, Tang Q, Peng X, Xu Y, Sun Z (2023) Effect of low protein diets supplemented with Sodium Butyrate, medium-chain fatty acids, or n-3 polyunsaturated fatty acids on the growth performance, Immune function, and Microbiome of Weaned piglets. *Int J Mol Sci* 24. <https://doi.org/10.3390/ijms242417592>
  39. Lippert K, Kedenko L, Antonielli L, Kedenko I, Gemeier C, Leitner M, Kautzky-Willer A, Paulweber B, Hackl E (2017) Gut microbiota dysbiosis associated with glucose metabolism disorders and the metabolic syndrome in older adults. *Beneficial Microbes* 8:545–556. <https://doi.org/10.3920/bm2016.0184>
  40. Loeffler JP, Picchiarelli G, Dupuis L, Gonzalez De Aguilar JL (2016) The role of skeletal muscle in amyotrophic lateral sclerosis. *Brain Pathol* 26:227–236. <https://doi.org/10.1111/bpa.12350>
  41. Margotta C, Fabbriozzi P, Ceccanti M, Cambieri C, Ruffolo G, D'Agostino J, Trolese MC, Cifelli P, Alfano V, Laurini C al (2023) Immune-mediated myogenesis and acetylcholine receptor clustering promote a slow disease progression in ALS mouse models. *Inflamm Regeneration* 43:19. <https://doi.org/10.1186/s41232-023-00270-w>
  42. Marino M, Papa S, Crippa V, Nardo G, Peviani M, Cheroni C, Trolese MC, Lauranzano E, Bonetto V, Poletti A et al (2015) Differences in protein quality control correlate with phenotype variability in 2 mouse models of familial amyotrophic lateral sclerosis. *Neurobiol Aging* 36:492–504. <https://doi.org/10.1016/j.neurobiolaging.2014.06.026>
  43. Martínez I, Perdicaro DJ, Brown AW, Hammons S, Carden TJ, Carr TP, Eskridge KM, Walter J (2013) Diet-induced alterations of host cholesterol metabolism are likely to affect the gut microbiota composition in hamsters. *Appl Environ Microbiol* 79:516–524. <https://doi.org/10.1128/aem.03046-12>
  44. Martínez I, Wallace G, Zhang C, Legge R, Benson AK, Carr TP, Moriyama EN, Walter J (2009) Diet-induced metabolic improvements in a hamster model of hypercholesterolemia are strongly linked to alterations of the gut microbiota. *Appl Environ Microbiol* 75:4175–4184. <https://doi.org/10.1128/aem.00380-09>
  45. Mazzini L, De Marchi F, Niccolai E, Mandrioli J, Amedei A (2021) Gastrointestinal Status and Microbiota Shaping in Amyotrophic lateral sclerosis: A New Frontier for Targeting? In: Araki T (ed) *Amyotrophic lateral sclerosis*. The Authors. City, Exon Publications Copyright
  46. Meissner F, Scheltema RA, Mollenkopf HJ, Mann M (2013) Direct proteomic quantification of the secretome of activated immune cells. *Sci (New York NY)* 340:475–478. <https://doi.org/10.1126/science.1232578>
  47. Murdock BJ, Famie JP, Piecuch CE, Pawlowski KD, Mendelson FE, Pieroni CH, Iniguez SD, Zhao L, Goutman SA, Feldman EL (2021) NK cells associate with ALS in a sex- and age-dependent manner. *JCI Insight* 6. <https://doi.org/10.1172/jci.insight.147129>
  48. Murdock BJ, Zhou T, Kashlan SR, Little RJ, Goutman SA, Feldman EL (2017) Correlation of Peripheral Immunity with Rapid Amyotrophic lateral sclerosis progression. *JAMA Neurol* 74:1446–1454. <https://doi.org/10.1001/jamaneurol.2017.2255>
  49. Nagpal R, Wang S, Solberg Woods LC, Seshie O, Chung ST, Shively CA, Register TC, Craft S, McClain DA, Yadav H (2018) Comparative Microbiome signatures and short-chain fatty acids in mouse, Rat, non-human primate, and human feces. *Front Microbiol* 9:2897. <https://doi.org/10.3389/fmicb.2018.02897>
  50. Nardo G, Iennaco R, Fusi N, Heath PR, Marino M, Trolese MC, Ferraiuolo L, Lawrence N, Shaw PJ, Bendotti C (2013) Transcriptomic indices of fast and slow disease progression in two mouse models of amyotrophic lateral sclerosis. *Brain* 136:3305–3332. <https://doi.org/10.1093/brain/awt250>
  51. Nardo G, Trolese MC, Tortorolo M, Vallarola A, Freschi M, Pasetto L, Bonetto V, Bendotti C (2016) New insights on the mechanisms of Disease Course variability in ALS from Mutant SOD1 mouse models. *Brain Pathol* 26:237–247. <https://doi.org/10.1111/bpa.12351>
  52. Niccolai E, Baldi S, Ricci F, Russo E, Nannini G, Menicatti M, Poli G, Taddei A, Bartolucci G, Calabrò AS al (2019) Evaluation and comparison of short chain fatty acids composition in gut diseases. *World J Gastroenterol* 25:5543–5558. <https://doi.org/10.3748/wjg.v25.i36.5543>
  53. Niccolai E, Di Pilato V, Nannini G, Baldi S, Russo E, Zucchi E, Martinelli I, Menicatti M, Bartolucci G, Mandrioli J et al (2021) The Gut Microbiota-Immunity Axis in ALS: A Role in Deciphering Disease Heterogeneity? *Biomedicines* 9. <https://doi.org/10.3390/biomedicines9070753>
  54. Niccolai E, Pedone M, Martinelli I, Nannini G, Baldi S, Simonini C, Di Gloria L, Zucchi E, Ramazzotti M, Spezia PG al (2024) Amyotrophic lateral sclerosis stratification: unveiling patterns with virome, inflammation, and metabolism molecules. *J Neurol* 271:4310–4325. <https://doi.org/10.1007/s00415-024-12348-7>
  55. Ota M, Matsuo J, Ishida I, Takano H, Yokoi Y, Hori H, Yoshida S, Ashida K, Nakamura K, Takahashi T al (2019) Effects of a medium-chain triglyceride-based ketogenic formula on cognitive function in patients with mild-to-moderate Alzheimer's disease. *Neurosci Lett* 690:232–236. <https://doi.org/10.1016/j.neulet.2018.10.048>
  56. Park JC, Im S-H (2020) Of men in mice: the development and application of a humanized gnotobiotic mouse model for microbiome therapeutics. *Exp Mol Med* 52:1383–1396. <https://doi.org/10.1038/s12276-020-0473-2>
  57. Pizzasegola C, Caron I, Daleno C, Ronchi A, Minoia C, Carri MT, Bendotti C (2009) Treatment with lithium carbonate does not improve disease progression in two different strains of SOD1 mutant mice. *Motor Neuron Dis* 10:221–228. Amyotrophic lateral sclerosis: official publication of the World Federation of Neurology Research Group on 10.1080/17482960902803440
  58. Priyadarshini M, Kotlo KU, Dudeja PK, Layden BT (2018) Role of short chain fatty acid receptors in intestinal physiology and pathophysiology. *Compr Physiol* 8:1091–1115. <https://doi.org/10.1002/cphy.c170050>
  59. Ren W, Wu Q, Deng L, Hu Y, Guo W, Ren N (2022) Simultaneous medium chain fatty acids production and process carbon emissions reduction in a continuous-flow reactor: re-understanding of carbon flow distribution. *Environ Res* 212:113294. <https://doi.org/10.1016/j.envres.2022.113294>
  60. Saerens SM, Verstrepen KJ, Van Laere SD, Voet AR, Van Dijkck P, Delvaux FR, Thevelein JM (2006) The *Saccharomyces cerevisiae* EHT1 and EEB1 genes encode novel enzymes with medium-chain fatty acid ethyl ester synthesis and hydrolysis capacity. *J Biol Chem* 281:4446–4456. <https://doi.org/10.1074/jbc.M512028200>
  61. Sagi H, Shibuya S, Kato T, Nakanishi Y, Tsuboi A, Moriya S, Ohno H, Miyamoto H, Kodama H, Shimizu T (2020) SOD1 deficiency alters gastrointestinal microbiota and metabolites in mice. *Exp Gerontol* 130:110795. <https://doi.org/10.1016/j.exger.2019.110795>
  62. Salonen A, Lahti L, Salojärvi J, Holtrop G, Korpela K, Duncan SH, Date P, Parquharson F, Johnstone AM, Lobley GE et al (2014) Impact of diet and individual variation on intestinal microbiota composition and fermentation products in obese men. *The ISME journal* 8: 2218–2230 <https://doi.org/10.1038/ismej.2014.63>
  63. Shi N, Li N, Duan X, Niu H (2017) Interaction between the gut microbiome and mucosal immune system. *Military Med Res* 4:14. <https://doi.org/10.1186/s40779-017-0122-9>
  64. Steyn FJ, Li R, Kirk SE, Tefera TW, Xie TY, Tracey TJ, Kelk D, Wimberger E, Garton FC, Roberts Let al et al (2020) Altered skeletal muscle glucose–fatty acid flux in amyotrophic lateral sclerosis. *Brain Commun* 2. <https://doi.org/10.1093/braincomms/fcaa154>
  65. Suzuki M, Takaishi S, Nagasaki M, Onozawa Y, Iino I, Maeda H, Komai T, Oda T (2013) Medium-chain fatty acid-sensing receptor, GPR84, is a proinflammatory receptor. *J Biol Chem* 288:10684–10691. <https://doi.org/10.1074/jbc.M112.420042>
  66. Trolese MC, Scarpa C, Melfi V, Fabbriozzi P, Sironi F, Rossi M, Bendotti C, Nardo G (2022) Boosting the peripheral immune response in the skeletal muscles improved motor function in ALS transgenic mice. *Mol Therapy: J Am Soc Gene Therapy* 30:2760–2784. <https://doi.org/10.1016/j.jymthe.2022.04.018>
  67. Vacca M, Celano G, Calabrese FM, Portincasa P, Gobetti M, De Angelis M (2020) The controversial role of human gut Lachnospiraceae. *Microorganisms* 8. <https://doi.org/10.3390/microorganisms8040573>
  68. Valbuena GN, Cantoni L, Tortorolo M, Bendotti C, Keun HC (2019) Spinal cord metabolic signatures in models of fast- and slow-progressing SOD1 (G93A) amyotrophic lateral sclerosis. *Front NeuroSci* 13:1276. <https://doi.org/10.3389/fnins.2019.01276>

69. Wu S, Yi J, Zhang YG, Zhou J, Sun J (2015) Leaky intestine and impaired microbiome in an amyotrophic lateral sclerosis mouse model. *Physiological Rep* 3. <https://doi.org/10.14814/phy2.12356>
70. Yokota A, Fukiya S, Islam KBMS, Ooka T, Ogura Y, Hayashi T, Hagio M, Ishizuka S (2012) Is bile acid a determinant of the gut microbiota on a high-fat diet? *Gut Microbes* 3:455–459. <https://doi.org/10.4161/gmic.21216>
71. Zagato E, Pozzi C, Bertocchi A, Schioppa T, Saccheri F, Guglietta S, Fosso B, Melocchi L, Nizzoli G, Troisi J al (2020) Endogenous murine microbiota member *Faecalibaculum rodentium* and its human homologue protect from intestinal tumour growth. *Nat Microbiol* 5:511–524. <https://doi.org/10.1038/s41564-019-0649-5>
72. Zhang Y, Ogbu D, Garrett S, Xia Y, Sun J (2021) Aberrant enteric neuromuscular system and dysbiosis in amyotrophic lateral sclerosis. *Gut Microbes* 13:1996848. <https://doi.org/10.1080/19490976.2021.1996848>

### Publisher's note

Springer Nature remains neutral with regard to jurisdictional claims in published maps and institutional affiliations.